http://dx.doi.org/10.21577/0103-5053.20190087

*J. Braz. Chem. Soc.*, Vol. 30, No. 9, 1807-1813, 2019
Printed in Brazil - ©2019 Sociedade Brasileira de Química

Article

# Layered Double Hydroxides with the Composition Mn/Al-$SO_4$-A (A = Li, Na, K; Mn:Al ca. 1:1) as Cation Exchangers

*Anne R. Sotiles,[a] Neffer A. G. Gomez,[a] Suelen C. da Silva[a] and Fernando Wypych*[*,a]*

[a]*Departamento de Química, Universidade Federal do Paraná, CP 19032, Jardim das Américas, 81531-980 Curitiba-PR, Brazil*

Hydrated Mn/Al-$SO_4$-A (A = Li, Na or K) layered double hydroxides with $M^{2+}$:$M^{3+}$ molar ratio close to 1:1 were synthesized by co-precipitation with increasing pH. All phases presented solvated alkali metals and sulfate as intercalated species. In the exchange reactions, when sulfate solutions of alkali metals were used, sodium could be partially replaced by potassium, and the same was true for the potassium phase, where potassium could be partially replaced by Na and Li, without removing the intercalated sulfate anions. This class of compounds, considered to be anion exchanger, can also exchange cations, which opens new perspectives for applications.

**Keywords:** layered double hydroxides, exchange reactions, shigaite, cation exchangers

## Introduction

Layered double hydroxides (LDHs) are materials with a generic composition $[M^{2+}_{1-x}M^{3+}_{x}(OH)_2](A^{n-})_{x/n}.yH_2O$, where $M^{2+}$ in the brucite-like structure is partially replaced by $M^{3+}$, generating an excess of positive charges, which are counterbalanced by the intercalation of hydrated anions. Normally crystalline materials can be obtained with $M^{2+}$:$M^{3+}$ molar ratios in the range of 2 to 4.

Although different anions can be intercalated between the LDHs layers,[1,2] the intercalation of sulfate are not so frequently reported, due specially to the system complexity.[3-8] In a recent work, Khaldi *et al.*[9] detected two different phases in the LDH Zn/Cr-$SO_4$ ($Zn^{2+}$:$Cr^{3+}$ = 2:1), which were dependent on the pH and washing procedure. During fast washing the basal distance of 11 Å was obtained and after extensive washing, the basal distance was reduced to 8.9 Å. The authors also observed that the 11 Å phase was rich in sulfate and contained sodium while the phase of 8.9 Å was poor in sulfate and devoid of sodium. The authors also reported that the basal parameters of these compounds were dependent on the drying process and relative air humidity, during samples manipulations.

The synthesis of Zn/Al and Zn/Cr ($Zn^{2+}$:$M^{3+}$ = 2:1)[10] also indicated several phases, with basal distances of 11 Å (d), 9.2 Å (d, r), 8.8 Å (d), 8.7 Å (r), 8.2 Å (d) and 7.1 Å (d) when different washing and drying conditions were applied (d and r represent the phase observed during dehydration and rehydration, respectively). All the phases were attributed to several degrees of sulfate hydration and interpolytype transitions during dehydration/rehydration and the lower basal spacing was attributed to grafting of sulfate to the LDH layers.

Another work[9] described the Zn:$M^{3+}$-$SO_4$ ($Zn^{2+}$:$M^{3+}$ = 2:1 and $M^{3+}$ = Al, Cr) system and explored the precipitation at acid and basic pH and also the hydrothermal treatment at 125 and 150 °C. Again, the phase of 10.9 Å was observed at room temperature, which after the hydrothermal treatment was transformed to a phase with a basal distance of 8.8 Å. In these samples, no sodium was detected and this change was attributed to interpolytype transitions.

LDH minerals intercalated with sulfate, with the ideal formula $(Na(H_2O)_6)[M^{2+}_6Al_3(OH)_{18}(SO_4)_2].6H_2O$, where $M^{2+}$ = Mg, Zn, Mn and Fe, respectively for the minerals motukoreaite,[11] natroglaucocerinite,[12] shigaite[13-15] and nikisherite[16] are also known. Iron green rust $NaFe^{II}_6Fe^{III}_3(SO_4)_2(OH)_{18}.12H_2O$ was also reported to have the same structure.[17] In these materials, the interlayer domains present the anion $[NaSO_4.SO_4(H_2O)_{12}]^{3-}$, where sodium cations are coordinated by six water molecules in an octahedral arrangement that compensates the cationic layer domains $[M^{2+}_6Al_3(OH)_{18}]^{3+}$. As only sulfate and alkali metal cations are available, the way to produce a neutral structure is to intercalate one sulfate anion and one sodium sulfate anion, which occurs in the mineral structures $\{[M^{2+}_6Al_3(OH)_{18}]^{3+}[(SO_4^{2-})(NaSO_4^{-}]^{3-}\}$.

*e-mail: wypych@ufpr.br

It is important to emphasize that most of the papers involving LDH indicated that this class of materials can exchange only anions and the present work proposes that these materials can also exchange cations, as recently proposed for LDH with $M^{2+}$:$M^{3+}$ molar rations of 2:1.[18] To contribute to research in this area we studied the synthesis of Mn/Al-$SO_4$-A (A = Na, K, Li), but instead of Zn:Al molar ratios of 2:1,[12-16] common for the minerals and synthetic LDH,[18] we investigated phases with molar ratios of 1:1. The aim was to investigate the exchange of the alkali metal without removing sulfate anions.

## Experimental

All the chemicals were of analytical grade (more than 99% purity) and were used without any treatment. In the synthesis of Mn/Al-$SO_4$-Na (Na-phase), co-precipitation with increasing pH was used. To 100 mL of type-I water (Milli-Q integral purification system: 18.2 MΩ cm) solutions containing 26.151 mmol of $MnSO_4.H_2O$, 13.079 mmol of $Al_2(SO_4)_3.16H_2O$ and 4.365 mmol of $Na_2SO_4$ were titrated with NaOH 1.5 mol $L^{-1}$ in a glass reactor operating at 90 °C, under flow of $N_2$ (pH was increased from 3.28 to 9.02). The materials were maintained at 90 °C for 120 h, centrifuged at 4000 rpm, washed several times with type-I water and dried at room temperature until constant weight.

In the synthesis of Mn/Al-$SO_4$-K (K-phase), 25.795 mmol of $MnSO_4.H_2O$, 12.895 mmol of $Al_2(SO_4)_3.16H_2O$ and 4.304 mmol of $K_2SO_4$ were titrated with KOH (pH was increased from 3.45 to 8.99) and the synthesis conditions were maintained constant. In the synthesis of Mn/Al-$SO_4$-Li (Li-phase), 26.506 mmol of $MnSO_4.H_2O$, 12.760 mmol of $Al_2(SO_4)_3.16H_2O$ and 4.366 mmol of $Li_2SO_4$ were titrated with LiOH (pH was increased from 3.47 to 8.98) and the synthesis conditions were maintained constant.

To exchange intercalated Na with K, an aqueous dispersion of the Na-phase was stirred with an excess of $K_2SO_4$ (three times the concentration of intercalated sodium) for 24 h at room temperature. To exchange intercalated K with Na and Li in K-phase, the same procedure was adopted, but using $Na_2SO_4$ and $Li_2SO_4$, respectively. To avoid contamination with carbonate, all the reactions were performed under flow of $N_2$ and after the reactions the materials were centrifuged at 4000 rpm, washed several times with type-I water and dried at room temperature until constant weight.

To expose the basal diffraction peaks in the X-ray diffraction (XRD) patterns, the samples were prepared before the drying process, using a drop of the last dispersion after centrifugation which was deposited on the sample holder and let to dry at room temperature. The XRD patterns were obtained using a Shimadzu XRD-6000 diffractometer with $CuK_\alpha$ radiation source of λ = 1.5418 Å, current of 30 mA, tension of 40 kV, dwell time of 2° $min^{-1}$ and step of 0.02 degrees.

The FTIR (Fourier transform infrared) spectra were obtained in the transmission mode in a Bio-Rad FTS 3500GX spectrometer in KBr discs. A total of 32 scans were accumulated from 400 to 4000 $cm^{-1}$, with resolution of 4 $cm^{-1}$.

To investigate the morphology and the qualitative chemical composition, scanning electron microscopy (SEM) images were acquired with an FEI Quanta 450 FEG electron microscope with AZ Tech software equipped with an X-ray energy dispersive spectroscopic analyzer using an SDD (silicon drift) detector. The samples were deposited on copper double-face tape, and after the EDS (energy dispersive X-ray spectroscopy) analysis, the samples were gold sputtered for SEM image acquisition.

The spectrometric determinations were carried out with a Thermo Scientific simultaneous axial view ICP OES (inductively coupled plasma optical emission spectrometry) spectrometer (model iCAP 6500) and the ThermoiTeVa Analyst version 1.2.0.30 program was used for data treatment. Two samples of the same composition were dissolved in a solution containing 1.0% (v/v) $HNO_3$, diluted when necessary and analyzed in duplicate. Average values were used in the compounds formulations.

Selected area electron diffraction (SAED) spectra were obtained with a JEOL JEM 1200 EX-II apparatus operating at 120 kV.

## Results and Discussion

The X-ray diffraction patterns of Na (Figure 1a), K (Figure 1c) and Li-phase (Figure 1f) were very similar to the phase obtained for the Zn/Cr-$SO_4$-Na reported by Khaldi *et al.*,[9] indexed as 2H structure (a = b = 5.49 Å, c = 22.06 Å).

Although the composition $M^{2+}$:$M^{3+}$ is close to 1:1, the Na-phase XRD pattern (Figure 1a) is very close to the Na-shigaite (a = b = 9.51 Å, c = 33.09 Å).[13-15]

Another possibility is to index the LDH as 1H polytype, although this composition sodium was not detected,[19] but according to the authors, there were two superlattice diffraction peaks in the region of 18-23° (in 2θ), which were confirmed in the SAED spectra (Figure 2) and also observed in the XRD patterns, indicating that this polytype was the most probable in the synthesized samples.

The cell parameters used to index the Na-phase were a = b = 5.49 Å and c = 11.03 Å. The difference between

these phases and ours is that the former had $M^{2+}$:$M^{3+}$ molar ratio of 2:1, while the present case had Mn:Al molar ratio of 1:1 (see ICP OES analysis, in Table 1). The basal distance of the K-phase was slightly expanded to 11.23 Å (Figure 1c) in comparison with the Na-phase, while in the Li-phase the basal distance was contracted to 10.90 Å. One main difference between the Na, K and Li-phases is the existence of three diffraction peaks in the region of 57-63° (in 2θ) for the Na-phase, while this region contains four diffraction peaks in the K and Li-phases, which indicates a probable reduction of the structural symmetry.

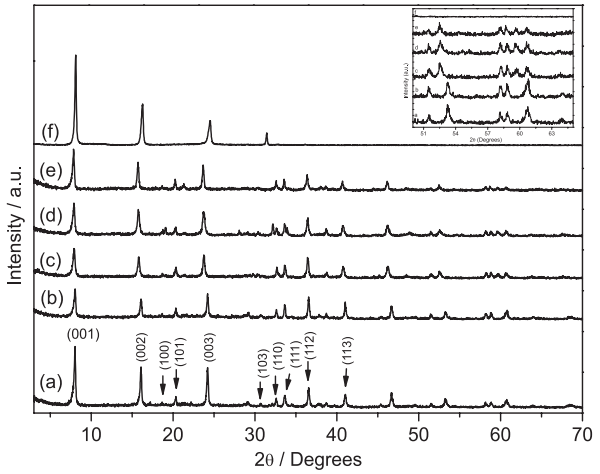


**Figure 1.** XRD patterns of Na-phase (a); after Na/K exchange (b); K-phase (c); after K/Na exchange (d); after K/Li exchange (e) and Li-phase (f) (oriented to expose basal peaks). Insert: expansion of the XRD in the range of 50 to 65° region.

After the exchange of Na with K (Figure 1b) and K with Na or Li (Figures 1d and 1e), the basal parameters remained almost the same as those of the parent material, which would indicate an unsuccessful reaction, but probably hydrated sulfate anion double layers defined the basal distance, with only a slight influence of the hydrated alkali cations. None of the phases presented any possible contaminations or reduced basal distances, as previously reported for dehydrated sulfate intercalated samples.[10,11,20] To confirm whether the samples basal distance would vary with the Mn:Al molar ratio, samples of Na, K and Li-shigaite were synthesized with the $M^{2+}$:$M^{3+}$ molar ratio of 2:1, using similar conditions as used for the 1:1 phases (Figure 3).[18]

The XRD patterns were very similar and the basal distances were close to the Mn:Al molar ratios of 1:1, within the techniques experimental error range (Mn:Al 1:1, Na = 11.03 Å, K = 11.23 Å and Li = 10.90 Å; Mn:Al 2:1, Na = 11.03 Å, K = 11.28 Å and Li = 10.88 Å). The position of the 100 peak remained the same (2θ ca. 18.65°), indicating the maintenance of the same a and b parameters.

The FTIR spectra of the 1:1 phases (Figure 4) were in agreement with the literature on sulfate intercalated in LDH[9,21] and layered hydroxide salt (LHS), like gordaite.[22]

Briefly in the Na-phase, the broad band at 3440 $cm^{-1}$ is attributed to the stretching of the O–H bonds of the LDH structure and physisorbed/intercalated water molecules. The band at 1654 $cm^{-1}$ is attributed to the water molecule bending.

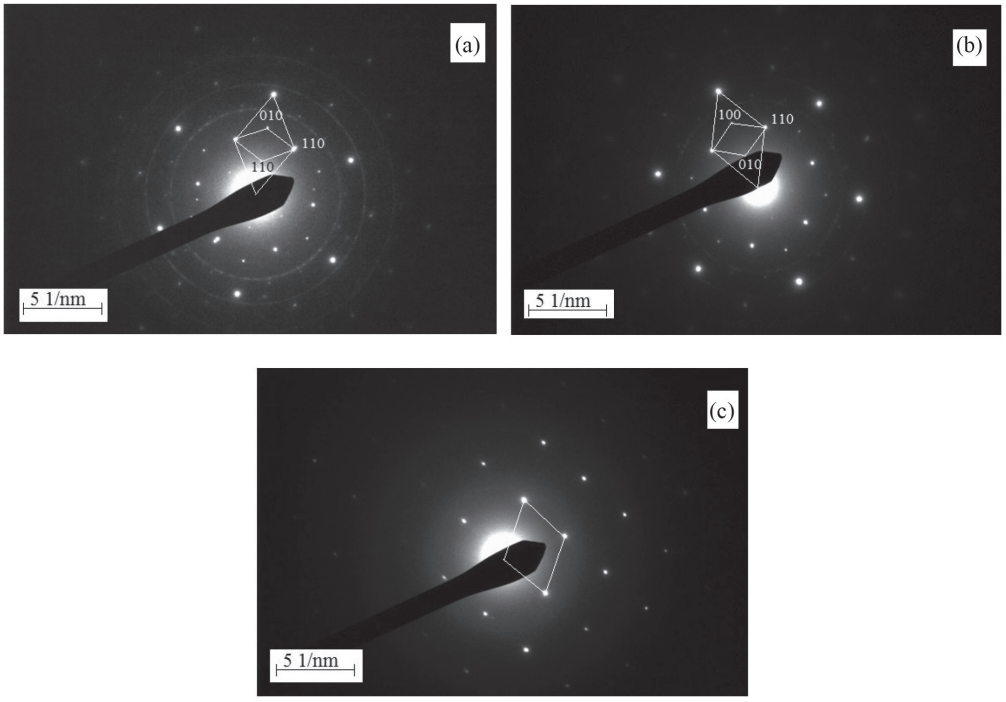


**Figure 2.** SAED spectra of Na (a); K (b) and Li-phase (c), indicating the lattice and superlattice spots.

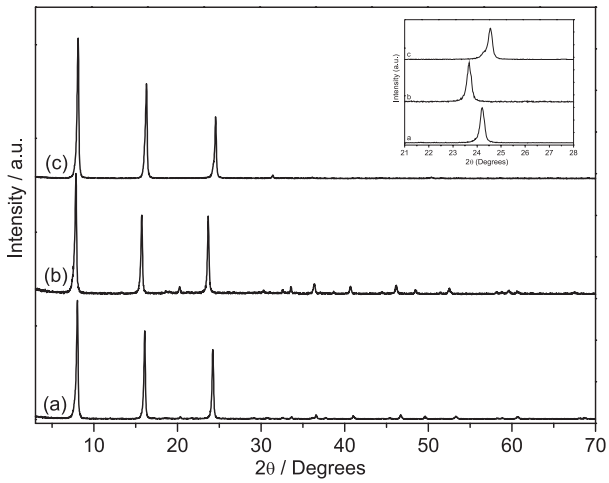


**Figure 3.** XRD patterns of Na (a); K (b) and Li-shigaite (c). The samples were oriented in the sample holder to expose basal peaks. Insert: expansion of the XRD in the region of the third basal peak.

The S–O bonds of sulfate were observed at 1108 $cm^{-1}$ ($\nu$3 = shoulder at 1065, 1140 and 1190 $cm^{-1}$), 960 ($\nu$1) and 608 $cm^{-1}$ ($\nu$4). As the $\nu$1 (region of 960 $cm^{-1}$) and $\nu$4 bands (region of 600 $cm^{-1}$) were also observed and sulfate is present in a tetrahedral distorted environment,[23,24] interacting with water molecules, these two anions can vibrate in-phase or out-of-phase, inducing two or three bands for the $\nu$3 mode, as indicated for sulfate green rusts, having almost identical environment.[25]

The M–O and M–OH bonds were detected at 770, 534, 470 and 420 $cm^{-1}$. The only small difference between the Na-phase (Figure 4a), K-phase (Figure 4c) and Li-phase (Figure 4f) was the splitting of the band at around 960 $cm^{-1}$ in the Na and Li-phases into two bands at around 945 and 975 $cm^{-1}$. The broadening and splitting of the bands at 1100 and 960 $cm^{-1}$ can probably be attributed to sulfate

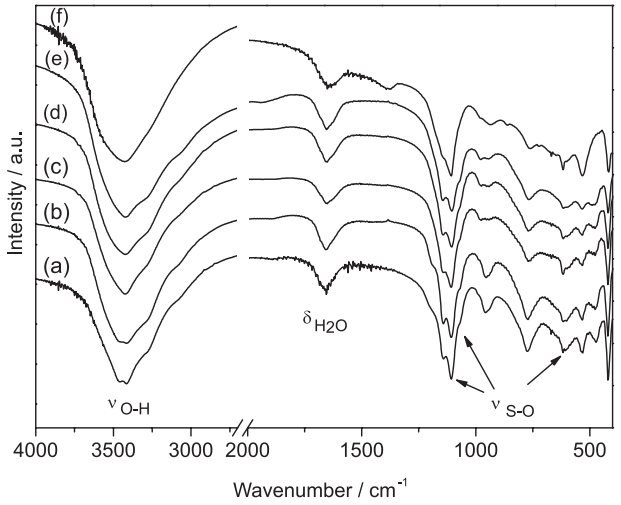


**Figure 4.** FTIR spectra of Na-phase (a); after Na/K exchange (b); K-phase (c); after K/Na exchange (d); after K/Li exchange (e) and Li-phase (f).

anions having reduced symmetries, due to the influence of the water molecules, sodium and the positively charged layers.[26] After the exchange reactions (Figures 4b, 4d, 4e), the spectra were similar to the parent materials.

The SEM images of the Na-phase (Figure 5a), after Na/K exchange (Figure 5b), K-phase (Figure 5c), after K/Na exchange (Figure 5d), after K/Li exchange (Figure 5e) and Li-phase (Figure 5f) presented the typical sub-micrometer size platelet-like particles with nanometer thicknesses.

All the other samples had a similar profile. After the exchange reactions, the crystals were smaller, probably due to the mechanical abrasion caused by the magnetic stirring. In the qualitative EDS spectra, all the major expected elements were present in the analyzed samples (not shown). The results of ICP OES indicated the compounds had composition close to the $M^{2+}$:$M^{3+}$ molar ratio used in the synthesis and only Na, K and Li were detected in the respective phases (Table 1).

To explain the presence of alkali metal and sulfate into the structure, the reduced composition can be formulated close to the ideal $Mn_{0.5}Al_{0.5}(OH)_2(SO_4)_{0.333}A_{0.167}$ (A = alkali metal), which in integral number would be $Mn_3Al_3(OH)_{12}(SO_4)_2A_1$. Looking to the formula, it is clear to see why the alkali metal is present in the structure since the unit $[Mn_3Al_3(OH)_{12}]^{3+}$ needs to be neutralized and only double negative charged sulfate are present. To neutralize the charged layers one $SO_4^{2-}$ and one $NaSO_4^-$ anions are necessary. In a generic view, the structure of the compound can be written as $[Mn_3Al_3(OH)_{12}]^{3+}[(SO_4)_2A_1]^{3-}\cdot nH_2O$ or $[Mn_3Al_3(OH)_{12}]^{3+}[(SO_4)(ASO_4)]^{3-}\cdot nH_2O$.

Only the Li-phase presented a lower content of lithium in comparison to the Na and K phases. The amounts of sulfate and hydroxide in the structure were obtained by difference, but the presence of O and S was detected by EDS (not shown), and OH and sulfate was also confirmed by FTIR. After the exchange reactions, about 39% of the Na was replaced by K in the Na-phase, 56% of the K was replaced by Na in the K-phase and 70% of the K was replaced by lithium in the K-phase, indicating that all the phases can exchange cations, although the first reactions were less favorable. We are currently studying longer exchange times and higher concentrations of salts in solution to try to totally substitute the intercalated cations, without removing the intercalated sulfate anions as well as the exchange of sulfate by carbonate exchanging simultaneously or preserving the alkali metal cations.

To investigate the structure of the samples, SAED patterns were obtained for some selected crystals of the Na (Figure 2a), K (Figure 2b) and Li phases (Figure 2c). As can be seen, the selected Na and K phases presented hexagonal patterns where the crystals were oriented perpendicular to the basal direction (along the [00l] axis). Both presented

very close a and b cell parameters, with sharp spots with a = 3.17 Å and $a(3)^{1/2} \times a(3)^{1/2}$ superlattice spots with d = 5.49 Å (Figures 2a and 2b).

These superlattice spots are expected to be present for the ordering of the metals in the layers of LDH with $M^{2+}$:$M^{3+}$ 2:1 molar ratios, but not for $M^{2+}$:$M^{3+}$ 1:1. The

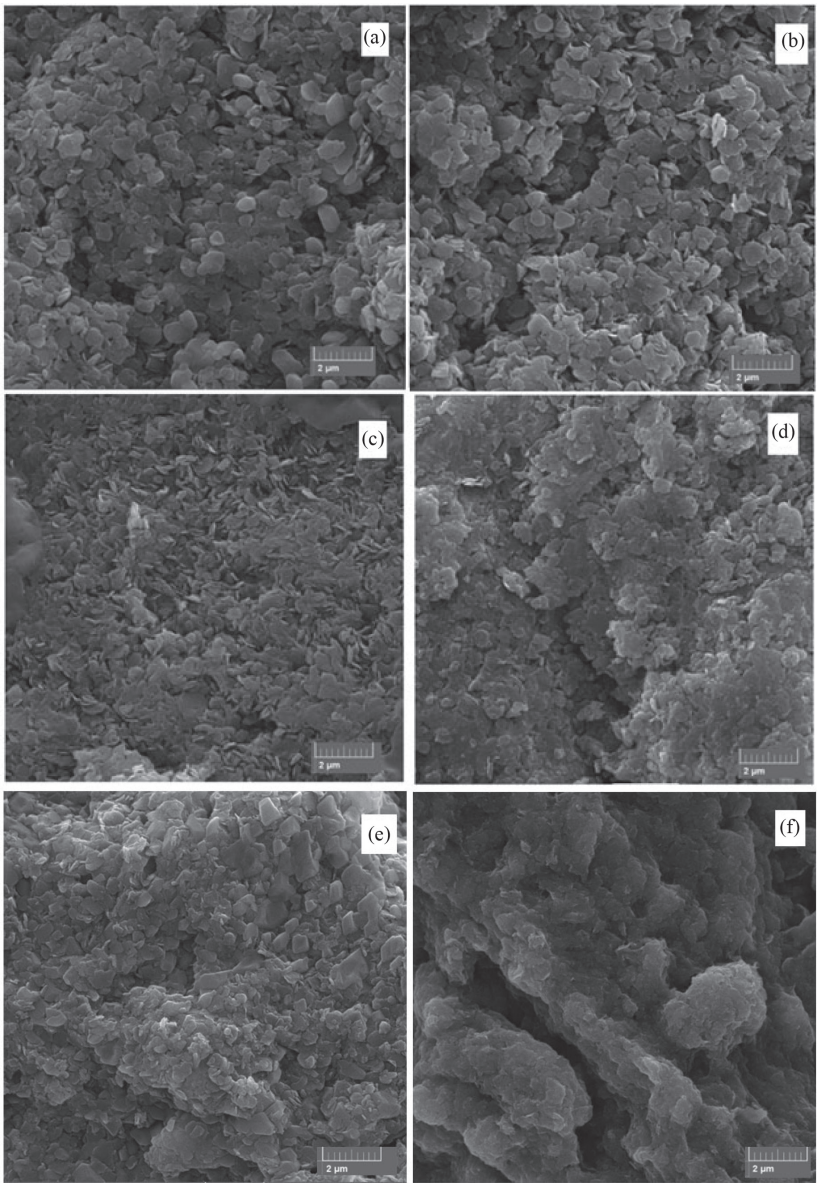


**Figure 5.** SEM images of the Na-phase (a); after Na/K exchange (b); K-phase (c); after K/Na exchange (d); after K/Li exchange (e) and Li phase (f).

**Table 1.** Compositions of the samples obtained by ICP OES

| Sample | Mn (x)[a] | Al (y)[a] | $SO_4$ (z)[a] | Alkali metal (w)[a] | Mn/Al[b] |
|---|---|---|---|---|---|
| Na-phase | 0.553 | 0.447 | 0.321 | Na = 0.195 | 1.24 |
| Na-phase/K | 0.512 | 0.488 | 0.322 | Na = 0.095; K = 0.061; Na + K = 0.156 | 1.05 |
| K-phase | 0.559 | 0.441 | 0.286 | K = 0.132 | 1.27 |
| K-phase/Na | 0.522 | 0.478 | 0.305 | K = 0.057; Na = 0.074; Na + K = 0.131 | 1.09 |
| K-phase/Li | 0.514 | 0.486 | 0.324 | K = 0.049; Li = 0.112; Na + Li = 0.161 | 1.06 |
| Li-Phase | 0.531 | 0.469 | 0.277 | Li = 0.084 | 1.13 |

[a]x,y,z,w: according to the LDH ideal formula, $Mn_xAl_y(OH)_2(SO_4)_zA_w$, where A means alkali metal; [b]Mn/Al: slightly higher than 1.0 is probably due to higher degree of hydration of the $Al_2(SO_4)_3 \cdot 16H_2O$ salt used in the synthesis.

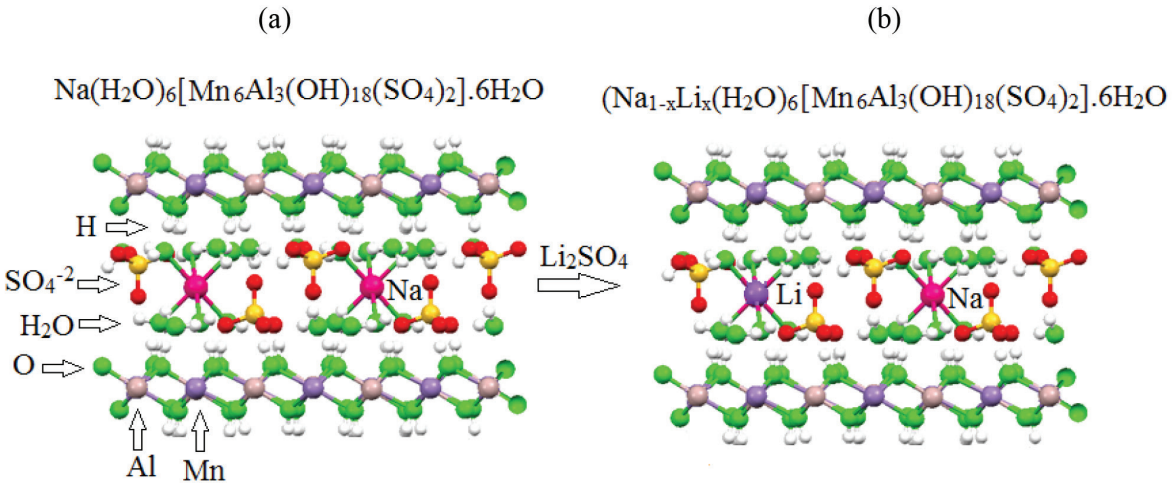


**Figure 6.** Schematic representation of (a) 1:1 $Mn^{2+}$:$Al^{3+}$ LDH structure intercalated with $Na^+$ and $SO_4^{2-}$; (b) the structure resulted from the topotactic partial exchange reactions of $Na^+$ with $Li^+$.

Li-phase did not present the superlattice spots (Figure 5c), due probably to the lower content of intercalated lithium (see Table 1). As expected, almost the same a and b cell parameters were also obtained for the samples after the exchange reactions (not shown), integrity (topotactic exchange reaction).

Figure 6 shows the schematic representation of the $Mn^{2+}$:$Al^{3+}$ 1:1 LDH structure intercalated with $SO_4^{2-}$ and $NaSO_4^-$ (also said, intercalated with $SO_4^{2-}$ and $Na^+$) and the structure resulted from the partial topotactic exchange reactions of $Na^+$ with $Li^+$ (equation 1), when the reaction was performed in the presence of $Li_2SO_4$ and under $N_2$ atmosphere, to avoid the presence of $CO_2$ and consequently carbonate anions in the solution/intercalated.

$$[Mn_3Al_3(OH)_{12}][(SO_4)_2Na)] + x/2\ Li_2SO_4 \longrightarrow [Mn_3Al_3(OH)_{12}][(SO_4)_2Na_{1-x}Li_x)] + x/2\ Na_2SO_4 \quad (1)$$

## Conclusions

Hydrated phases of Mn/Al-$SO_4$-A (A = Na, K, Li; Mn:Al = 1:1) were synthesized by co-precipitation with increasing pH. All the samples were evaluated by XRD, presenting patterns starting with series of basal peaks, typical of materials with layered structures. No phases other than 11 Å were detected after extensive washing and drying under air.

After the exchange of Na with K and K with Na or Li, the a and b cell parameters were maintained almost constant in all samples, and only small variations were observed in the basal parameters, indicating that even after partial substitution of the alkali metal, the double layer of hydrated sulfate anions was responsible for the basal distance.

SAED patterns of the Na and K phase presented $a(3)^{1/2} \times a(3)^{1/2}$ superstructure, while the Li phase presented only the basic a × b hexagonal structure projection. After the exchange reactions, SAED patterns also showed maintenance of a and b parameters, indicating the layers' structural integrity after the reactions.

SEM and EDS indicated platelet-like particle morphology in all the samples, expected for the layered double hydroxides.

The ICP OES measurements indicated that the composition was close to the $M^{2+}$:$M^{3+}$ molar ratio used in the synthesis, indicating successful synthesis of Al rich LDH, with the ideal formula $[Mn_3Al_3(OH)_{12}]^{3+}[(SO_4)_2A_1]^{3-}\cdot nH_2O$ or $[Mn_3Al_3(OH)_{12}]^{3+}[(SO_4)(ASO_4)]^{3-}\cdot nH_2O$ (A = $Li^+$, $Na^+$ or $K^+$).

To confirm that the synthesized materials had similar structure as Na-shigaite (Mn:Al, 2:1) and can be stable in the presence of other alkali metals, Na, K and Li phases were synthesized and the similarities were confirmed.

Although the synthesized samples belong to the layered double hydroxide family, typical anion exchangers, the proposed reaction occurs just by replacing the alkali metal in the interlayer anions without replacing sulfate. This cation exchange capacity expands the applications of this class of compounds.

To give more information about the structure and thermodynamics properties of the exchange reactions of the minerals with the composition $(A^+(H_2O)_6)[M^{2+}{}_6Al_3(OH)_{18}(SO_4)_2]\cdot 6H_2O$ ($M^{2+}$ = Mg, Zn and $A^+$ = Na, K), *ab initio* calculations were performed.[27]

## Acknowledgments

This study was financed in part by the Coordenação de Aperfeiçoamento de Pessoal de Nível Superior

(CAPES), Brazil, Finance Code 001, Conselho Nacional de Desenvolvimento Científico e Tecnológico (CNPq), projects 303846/2014-3, 400117/2016-9 and the Financiadora de Estudos e Projetos (FINEP). A. R. S., N. A. G. G. and S. C. S. thank CAPES for the PhD scholarship. Loana Mara Baika and Prof Marco Tadeu Grassi are also aknowledged for the ICP OES analysis.

## References

1. Crepaldi, E. L.; Pavan, P. C.; Valim, J. B.; *J. Braz. Chem. Soc*. **2000**, *11*, 64.
2. Jaerger, S.; Zawadzki, S. F.; Leuteritz, A.; Wypych, F.; *J. Braz. Chem. Soc*. **2017**, *28*, 2391.
3. Nickel, E. H.; Clarke, R. M.; *Am. Mineral*. **1976**, *61*, 366.
4. Nickel, E. H.; Wildman, J. E.; *Mineral. Mag.* **1976**, *44*, 333.
5. Miyata, S.; Okada, A.; *Clays Clay Miner*. **1977**, *25*, 14.
6. Bish, D. L.; *Bull. Mineral*. **1980**, *103*, 170.
7. Bish, D. L.; Livingstone, A.; *Mineral. Mag.* **1981**, *44*, 339.
8. El Malki, K.; de Roy, A.; Besse, J. P.; *Eur. J. Solid State Inorg. Chem.* **1989**, *26*, 339.
9. Khaldi, M.; de Roy, A.; Chaouch, M.; Besse, J. P.; *J. Solid State Chem.* **1997**, *130*, 66.
10. Radha, S.; Antonyraj, C. A.; Kamath, P. V.; Kannan, S.; *Z. Anorg. Allg. Chem.* **2010**, *636*, 2658.
11. Rodgers, K. A.; Chisholm, J. E.; Davis, R. J.; Nelson, C. S.; *Mineral. Mag.* **1977**, *41*, 389.
12. Witzke, T.; Pöllmann, H.; Vogel, A.; *Z. Kristallogr.* **1995**, *Suppl. Issue 9*, 2522.
13. Cooper, M. A.; Hawthorne, F. C.; *Can. Mineral.* **1996**, *34*, 91.
14. Peacor, D. R.; Dunn, P. J.; Kato, A.; Wicks, J. J.; *Neues Jahrb. Mineral., Monatsh.* **1985**, 453.
15. Pring, A.; Slade, P. G.; Birch, W. D.; *Mineral. Mag.* **1992**, *56*, 417.
16. Huminicki, D. M. C.; Hawthornes, F. C.; *Can. Mineral*. **2003**, *41*, 79.
17. Christiansen, B. C.; Balic-Zunic, T.; Petit, P.-O.; Frandsen, C.; Mørup, S.; Geckeis, H.; Katerinopoulou, A.; Stipp, S. L. S.; *Geochim. Cosmochim. Acta* **2009**, *73*, 3579.
18. Sotiles, A. R.; Baika, L. M.; Grassi, M. T.; Wypych, F.; *J. Am. Chem. Soc.* **2019**, *141*, 531.
19. Radha, S.; Kamat, P. V.; *Inorg. Chem*. **2013**, *52*, 4834.
20. Mostarih, R.; de Roy, A.; *J. Phys. Chem. Solids* **2006**, *67*, 1058.
21. Li, F.; Liu, X.; Yang, Q.; Liu, J.; Evans, D. G.; Duan, X.; *Mater. Res. Bull.* **2005**, *40*, 1244.
22. Maruyama, S. A.; Krause, F.; Tavares, S. R.; Leitão, A. A.; Wypych, F.; *Appl. Clay Sci*. **2017**, *146*, 100.
23. Peak, D.; Ford, R. G.; Sparks, D. L.; *J. Colloid Interface Sci.* **1999**, *218*, 289.
24. Xuefeng W.; Lester, A.; *J. Phys. Chem. A* **2006**, *110*, 10035.
25. Zegeye, A.; Ona-Nguema, G.; Carteret, C.; Huguet, L.; Abdelmoula, M.; Jorand, F.; *Geomicrobiol. J.* **2005**, *22*, 389.
26. Lane, M. D.; *Am. Mineral.* **2007**, *92*, 1.
27. Moraes, P. I. R.; Wypych, F.; Leitão, A. A.; *J. Phys. Chem. C* **2019**, *123*, 9838.

*Submitted: January 7, 2019*
*Published online: May 9, 2019*

This is an open-access article distributed under the terms of the Creative Commons Attribution License.